Molecular Ecology (2008) **17**, 3062–3077 doi: 10.1111/j.1365-294X.2008.03815.x

Relative information content of polymorphic microsatellites and mitochondrial DNA for inferring dispersal and population genetic structure in the olive sea snake, *Aipysurus laevis*

V. LUKOSCHEK,*† M. WAYCOTT* and J. S. KEOGH‡
*School of Marine and Tropical Biology, James Cook University, Townsville, Qld 4811, Australia, †CRC Reef Research Centre, Townsville, Qld 4810, Australia, ‡School of Botany and Zoology, The Australian National University, Canberra, ACT, 0200, Australia

Abstract

Polymorphic microsatellites are widely considered more powerful for resolving population structure than mitochondrial DNA (mtDNA) markers, particularly for recently diverged lineages or geographically proximate populations. Weaker population subdivision for biparentally inherited nuclear markers than maternally inherited mtDNA may signal male-biased dispersal but can also be attributed to marker-specific evolutionary characteristics and sampling properties. We discriminated between these competing explanations with a population genetic study on olive sea snakes, *Aipysurus laevis*. A previous mtDNA study revealed strong regional population structure for *A. laevis* around northern Australia, where Pleistocene sea-level fluctuations have influenced the genetic signatures of shallow-water marine species. Divergences among phylogroups dated to the Late Pleistocene, suggesting recent range expansions by previously isolated matrilines. Fine-scale population structure within regions was, however, poorly resolved for mtDNA. In order to improve estimates of fine-scale genetic divergence and to compare population structure between nuclear and mtDNA, 354 olive sea snakes (previously sequenced for mtDNA) were genotyped for five microsatellite loci. *F* statistics and Bayesian multilocus genotype clustering analyses found similar regional population structure as mtDNA and, after standardizing microsatellite *F* statistics for high heterozygosities, regional divergence estimates were quantitatively congruent between marker classes. Over small spatial scales, however, microsatellites recovered almost no genetic structure and standardized *F* statistics were orders of magnitude smaller than for mtDNA. Three tests for male-biased dispersal were not significant, suggesting that recent demographic expansions to the typically large population sizes of *A. laevis* have prevented microsatellites from reaching mutation-drift equilibrium and local populations may still be diverging.

Keywords: assignment test, *F* statistics, gender biased dispersal, gene flow, mutations, sea snakes

Received 21 February 2008; revision received 12 April 2008; accepted 18April 2008

Introduction

Population genetic structures of species reflect both historical and contemporary processes (Balloux & Lugon-Moulin 2002); however, the relative effects of past vs. present processes can be challenging to tease apart, particularly when population structure is inferred from one class of genetic marker. Mitochondrial DNA (mtDNA) predominantly provides information about historical processes for intraspecific matrilineal relationships but may also allow insights into the importance of ongoing gene flow (Avise 2000). However, inferences from mtDNA data alone suffer from the well-known limitations of single-locus mitochondrial gene trees. The maternally inherited haploid mitochondrial genome has a fourfold smaller effective population size than nuclear markers, enhancing the effects of genetic drift

Correspondence: Vimoksalehi Lukoschek, Department Ecology and Evolutionary Biology, University of California, Irvine, Irvine, CA, 92697–2525, USA. Fax: 1-949-824-2181; E-mail: v.lukoschek@uci.edu

in subdivided populations and resulting in more rapid fixation or loss of alleles and stronger population subdivision at mitochondrial than nuclear loci (Birky *et al*. 1983). This effect is enhanced if migration is biased towards males but also holds in the absence of male-biased dispersal (Birky *et al*. 1983). In addition, while overall mutation rates tend to be higher for the mitochondrial than nuclear genome (Brown *et al*. 1979), much of the mitochondrial genome is protein coding and potentially under selection (Ballard & Kreitman 1995) and may not always evolve sufficiently rapidly to infer levels of contemporary gene flow (Angers & Bernatchez 1998).

Over the last decade, microsatellites have become the most commonly used nuclear markers in population genetic studies for a number of reasons (Estoup & Angers 1998). Microsatellites are biparentally inherited and most loci appear to be selectively neutral and accumulate mutations rapidly (Balloux & Lugon-Moulin 2002). Polymorphic microsatellites typically have high information content and are therefore expected to provide stronger discriminatory power for resolving population structure than mtDNA, allozymes or single copy nuclear DNA (scnDNA) (Goudet *et al*. 1996; Buonaccorsi *et al*. 1999). However, studies comparing genetic structures based on microsatellite and mitochondrial markers have documented varying patterns of congruence between marker classes: microsatellites have proved more powerful than mtDNA for resolving population structure in some cases (Angers & Bernatchez 1998; Wirth & Bernatchez 2001; Johnson *et al*. 2003) but not others (Pardini *et al*. 2001; Keeney *et al*. 2005), while broadly similar patterns or levels of population subdivision have also been found (Lehman *et al*. 1997; Allendorf & Seeb 2000; Natoli *et al*. 2004). Studies documenting weaker population subdivision for nuclear than mitochondrial markers often attribute these discrepancies to male-biased dispersal (Karl *et al*. 1992; Castella *et al*. 2001; Eizerik *et al*. 2001; Keeney *et al*. 2005). Yet Buonaccorsi *et al*. (2001) showed that differences in the magnitude of estimated population subdivision from nuclear and mitochondrial markers could be accounted for entirely by differences in effective population sizes and polymorphism on F_{ST} estimates.

As such, gender-biased dispersal is best regarded as a testable hypothesis when weaker population subdivision is found for nuclear than mitochondrial markers. Ideally, evidence for gender-biased dispersal would come directly from field studies (Keogh *et al*. 2007); however, field-based estimates of dispersal are notoriously difficult to obtain for many taxa. Fortunately, gender-biased dispersal can be tested using genetic data from microsatellites (Favre *et al*. 1997; Rassmann *et al*. 1997; Balloux *et al*. 1998; Mossman & Waser 1999) and mtDNA (FitzSimmons *et al*. 1997a; O'Corry-Crowe *et al*. 1997; Escorza-Trevino & Dizon 2000; Pardini *et al*. 2001). When direct tests of the molecular data fail to support gender-biased dispersal, discrepancies in levels of population subdivision recovered by nuclear and mitochondrial markers must be reconciled with the evolutionary characteristics and sampling properties of the marker-classes (Birky *et al*. 1983; Buonaccorsi *et al*. 2001), such as marker-specific mutation rates, modes of inheritance, and high variances in F_{ST} estimates (particularly for mtDNA) (Buonaccorsi *et al*. 2001). In addition, allele size homoplasy probably occurs at most microsatellite loci (Estoup *et al*. 2002), resulting in underestimated divergences between populations isolated over longer temporal and/or large spatial scales (Rousset 1996; Estoup *et al*. 2002). High within-group heterozygosities also reduce estimates of between-group divergence and may result in underestimated divergences (Hedrick 1999), particularly when migration rates are low (Balloux *et al*. 2000). Recently described methods for standardizing divergence estimates (Hedrick 2005; Meirmans 2006) provide one means of addressing this issue.

Geographically proximate populations with shallow evolutionary histories typify the set of circumstances where highly polymorphic microsatellite markers are expected to consistently outperform slowly evolving markers (Takahashi & Nei 1996). This expectation has been supported by empirical studies: microsatellites have resolved fine-scale population structures for marine (Angers & Bernatchez 1998; Shaw *et al*. 1999) and terrestrial organisms (Estoup *et al*. 1995; Queney *et al*. 2001) previously thought to be uniform based on mtDNA or allozymes. In evolutionarily recent times, Pleistocene processes have profoundly influenced the genetic signatures of organisms in a wide variety of ecosystems around the world (Hewitt 2000). In northern Australia, Pleistocene glaciation cycles and associated sea level fluctuations shifted the distributions of shallow-water marine habitats and changed the distributions and patterns of connectivity of tropical marine species in this region (Davies 1994; Lukoschek *et al*. 2007b). Taxa likely to have been most strongly affected are obligate shallow-water species with low dispersal potential. One such taxonomic group is the hydrophiine sea snakes, which occur primarily in shallow-water marine habitats (< 200 m deep). Marine hydrophiine species tend to have highly aggregated distributions (Lukoschek *et al*. 2007a) and all are viviparous (Heatwole 1999); thus, hydrophiine sea snakes potentially have limited dispersal capabilities compared to many marine taxa that have dispersive larval stages (Lukoschek *et al*. 2007a).

The olive sea snake, *Aipysurus laevis*, is the most common reef-associated (occurring primarily on coral reefs but also in inter-reef habitats) hydrophiine sea snake species in Australian waters. It is also the only marine hydrophiine species for which population genetic information is available (Lukoschek *et al*. 2007b). Based on mtDNA, Lukoschek *et al*. (2007b) documented striking hierarchical population structure for *A. laevis* throughout northern Australian waters. There was strong regional genetic subdivision (pairwise F_{ST}: 0.393–0.437; Φ_{ST}: 0.510–0.787), and although not

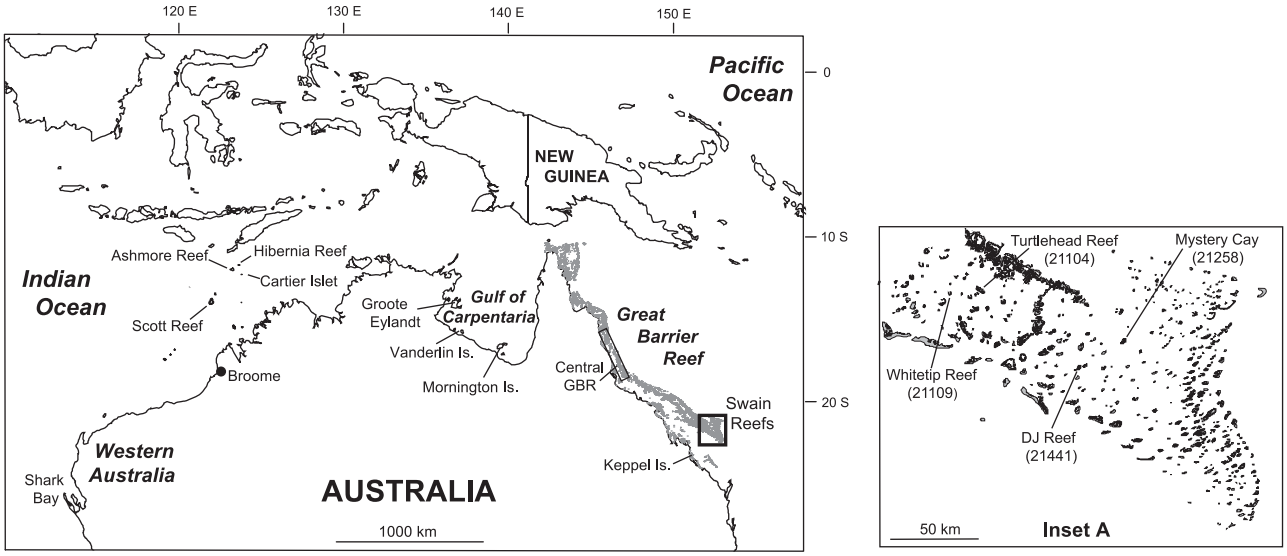

Fig. 1 Map indicating 14 locations from where *Aipysurus laevis* tissue samples were collected and other key locations mentioned in the text. Inset A: locations of four reefs sampled in the Swain Reefs. [Correction added after online publication 5 June 2008: the word '(underlined)' and the sentence 'Bold lines connecting Swain Reefs and Keppel Island indicate distances measured across shallow water habitat used as indicator Matrix in partial Mantel test for Great Barrier Reef' were deleted from the figure legend.]

unequivocal, multiple lines of evidence supported west-to-east range expansion following the last glacial maximum ~11 000 years ago (Lukoschek *et al*. 2007b). Phylogenetic reconstruction indicated that Western Australia (WA) had haplotypes ancestral to those found in the Gulf of Carpentaria (GoC) and Great Barrier Reef (GBR). In addition, WA had much higher genetic diversity than the GBR and GoC (Lukoschek *et al*. 2007b). Within regions, levels of gene flow reflected the connectivity afforded by regional habitat types, and provided evidence that deep water acts as a barrier to dispersal for *A. laevis.* Nonetheless, population structure among reefs in close proximity was poorly resolved, despite ecological evidence that these reefs may harbour discrete aggregations of *A. laevis* (Lukoschek *et al*. 2007a).

In order to determine whether the pattern of strong hierarchical population subdivision among *A. laevis* matrilines also occurs at biparentally inherited nuclear markers, and to resolve fine-scale patterns of gene flow within regions, species-specific microsatellite loci were developed (Lukoschek *et al*. 2005) and used to genotype the same individuals previously used for mtDNA analyses. We were interested in testing two hypotheses: (i) that polymorphic microsatellite markers are better able to resolve fine-scale patterns of population subdivision and gene flow than mtDNA; and (ii) west-to-east range expansion (see Lukoschek *et al*. 2007b for details of alternative hypotheses). As microsatellites recovered much weaker fine-scale genetic divergence than mtDNA, we also tested the hypothesis of male-biased dispersal. We evaluate these hypotheses in terms of the spatial and temporal scales at which microsatellites and mtDNA were most informative for inferring population subdivision and dispersal for *A. laevis*, focusing on the different evolutionary characteristics and sampling properties of the marker classes.

Materials and methods

Sampling design and genotyping

The same 354 *Aipysurus laevis* individuals (148 females, 199 males and 7 samples not sexed) previously sequenced for a 725-bp fragment of the mtDNA ND4-tRNA region (Lukoschek *et al*. 2007b) were genotyped for five species-specific polymorphic microsatellite loci using polymerase chain reaction (PCR) and screening protocols described in Lukoschek *et al*. (2005). Approximately 20% of samples were PCR-amplified and electrophoresed more than once to evaluate repeatability in scoring. The hierarchical sampling design comprised 14 locations in three regions (GBR, GoC, WA) from most of *A. laevis*' range around northern Australia (Fig. 1). Sample sizes for each location ranged from eight to 54 individuals (Table 1), with the exception of Broome (WA) where only one sample was obtained and was therefore excluded from some analyses.

Statistical analyses

Genetic variation and Hardy–Weinberg equilibrium. Microsatellite genotypes were determined as described in Lukoschek *et al*. (2005). Twenty-four snakes missing data at more than one locus were excluded from analyses. Numbers of alleles per locus, observed and expected heterozygosities,

Table 1 Summary statistics for six microsatellite loci screened for *Aipysurus laevis* in 13 locations and three geographical regions. Abbreviations are as follows: number of individuals (*N*), number of alleles observed per locus (*Na*), observed (H_O) and expected (H_E) heterozygosities, Wright's fixation index (F_{IS}). F_{IS} values in bold indicate significant departures from Hardy–Weinberg proportions. Bold values with one asterisk (*) were significant at $P < 0.05$ and bold values with double dagger (‡) were significant after sequential Bonferroni correction ($P < 0.0083$)

	AL106_d11	AL105_c4	AL28_h4	AL104_f6	AL093	All loci
Great Barrier Reef						
Keppel Island						
N	45	45	45	39	44	45
Na	2	3	2	5	11	4.6 (23)
H_O	0.022	0.311	0.511	0.333	0.841	0.404
H_E	0.022	0.364	0.437	0.603	0.869	0.459
F_{IS}	0.000	**0.156***	–0.159	**0.457‡**	**0.043‡**	
21104 Turtlehead Reef						
N	35	35	35	34	30	35
Na	2	3	2	7	10	4.8 (24)
H_O	0.029	0.229	0.257	0.118	0.833	0.293
H_E	0.082	0.275	0.474	0.649	0.858	0.467
F_{IS}	**0.660***	0.182	**0.469‡**	**0.824‡**	0.045	
21109 Whitetip Reef						
N	39	39	39	38	39	39
Na	3	3	2	8	10	5.2 (26)
H_O	0.154	0.359	0.538	0.500	0.897	0.490
H_E	0.144	0.347	0.453	0.575	0.858	0.475
F_{IS}	–0.058	–0.022	–0.177	**0.143***	–0.033	
21441 D-J Reef†						
N	34	34	34	19	34	34
Na	3	3	2	5	12	5.0 (25)
H_O	0.088	0.176	0.324	0.737	0.765	0.418
H_E	0.085	0.189	0.375	0.713	0.868	0.446
F_{IS}	–0.021	0.081	0.152	–0.006	0.133	
21258 Mystery Cay						
N	38	39	39	34	37	39
Na	2	3	2	7	11	5.0 (25)
H_O	0.026	0.308	0.436	0.353	0.973	0.419
H_E	0.026	0.272	0.416	0.460	0.877	0.410
F_{IS}	–0.013	–0.119	–0.035	**0.247***	–0.096	
Central GBR						
N	8	8	8	7	8	8
Na	1	3	2	4	8	3.6 (18)
H_O	0.000	0.250	0.750	0.286	0.875	0.432
H_E	0.000	0.227	0.469	0.459	0.844	0.400
F_{IS}	N/A	–0.037	–0.556	0.442	0.03	
All GBR locations						
N	199	200	200	171	192	200
Na	4	3	2	11	14	6.8 (34)
H_O	0.060	0.280	0.435	0.374	0.865	0.403
H_E	0.069	0.296	0.437	0.610	0.880	0.458
F_{IS}	0.122	0.057	0.007	**0.389‡**	0.020	
Gulf of Carpentaria						
Mornington Island						
N	6	6	6	6	6	6
Na	4	2	2	3	5	3.2 (16)
H_O	0.500	0.500	0.500	0.500	0.833	0.567
H_E	0.417	0.375	0.375	0.569	0.778	0.503
F_{IS}	–0.053	–0.25	–0.25	0.211	0.02	

Table 1 *Continued*

	AL106_d11	AL105_c4	AL28_h4	AL104_f6	AL093	All loci
Vanderlin Island						
N	34	34	33	33	34	34
Na	5	3	2	8	12	6.0 (30)
H_O	0.382	0.471	0.273	0.515	0.765	0.481
H_E	0.377	0.441	0.410	0.782	0.863	0.575
F_{IS}	0.001	–0.053	0.348	**0.355**‡	0.129	
Groote Eylandt						
N	15	15	15	14	14	15
Na	3	4	2	4	9	4.4 (22)
H_O	0.067	0.400	0.400	0.214	0.929	0.402
H_E	0.238	0.389	0.444	0.671	0.852	0.519
F_{IS}	**0.736**‡	0.006	0.134	**0.700**‡	–0.053	
All GoC locations						
N	55	55	54	53	54	55
Na	6	4	2	8	12	6.40 (32)
H_O	0.291	0.455	0.333	0.434	0.815	0.466
H_E	0.334	0.425	0.417	0.739	0.863	0.555
F_{IS}	0.137	–0.061	0.210	**0.421**‡	0.065	
Western Australia*						
Ashmore Reef						
N	30	33	33	28	33	33
Na	3	5	2	11	8	5.8 (29)
H_O	0.600	0.394	0.485	0.679	0.848	0.601
H_E	0.551	0.464	0.478	0.846	0.845	0.637
F_{IS}	–0.072	0.166	0	**0.216***	0.011	
Hibernia Reef						
N	9	8	9	8	9	9
Na	3	2	2	7	6	4.0 (20)
H_O	1.000	0.375	0.333	0.625	1.000	0.667
H_E	0.611	0.305	0.475	0.781	0.790	0.592
F_{IS}	**–0.600***	–0.167	0.351	0.263	–0.210	
Cartier Islet						
N	9	9	9	9	9	9
Na	3	4	2	7	7	4.6 (23)
H_O	0.778	0.667	0.556	0.667	1.000	0.733
H_E	0.586	0.636	0.401	0.796	0.778	0.640
F_{IS}	–0.273	0.010	–0.333	0.220	–0.231	
Scott Reef						
N	22	22	19	22	22	23
Na	3	5	2	8	11	5.8 (29)
H_O	0.455	0.636	0.579	0.591	0.682	0.589
H_E	0.528	0.717	0.450	0.780	0.861	0.667
F_{IS}	0.162	0.135	–0.261	0.264	**0.230**‡	
All WA locations						
N	71	73	71	68	74	75
Na	3	6	2	12	11	6.8 (34)
H_O	0.620	0.493	0.507	0.632	0.824	0.615
H_E	0.563	0.592	0.495	0.840	0.872	0.673
F_{IS}	–0.094	**0.174***	–0.017	**0.254**‡	0.062	
All locations¶						
N	325	328	325	292	320	330
Na	6	6	2	14	14	8.4 (42)
H_O	0.222	0.357	0.434	0.445	0.847	0.461
H_E	0.263	0.399	0.465	0.744	0.881	0.550
F_{IS}	**0.158**‡	**0.107**‡	0.069	**0.403**‡	0.041	

*Broome individual not shown. N/A, F_{IS} could not be calculated because H_O and H_E were zero. Significant LD after Bonferroni correction between †AL28_h4 vs. AL093; §AL105_c4 vs. AL104_f6; ¶AL106_d11 vs. AL104_f6; AL106_d11 vs. AL105 _c4; AL28_h4 vs. AL104_f6; AL105 _c4 vs. AL104_f6.

deviations from Hardy–Weinberg equilibria (HWE), and exact tests of linkage disequilibrium (LD) between pairs of loci were calculated for each location, each region, and across all samples using GENEPOP 3.4 (Raymond & Rousset 1995). Unbiased estimators of significance levels were calculated using the Markov chain algorithm of Guo & Thompson (1992). Markov chains were run for 2 million steps (10 000 dememorization step intervals) before comparing observed and permuted values. Unbiased estimates of allelic richness and gene diversity were calculated for each region to allow direct comparisons (Goudet 2001). Allelic richness, standardized to a sample size of 20, and gene diversity (Nei 1987), weighted by regional sample size, were calculated in FSTAT 2.9. Tests of significance were conducted using the 'compare-groups' option in FSTAT 2.9 and evaluated using 15 000 permutations.

Population subdivision from F *statistics.* Hierarchical AMOVA estimated three variance components (among regions, among locations within regions, and within locations) using the infinite allele model (IAM – F_{ST}), and stepwise mutation model (SMM – R_{ST}) (Slatkin 1995). AMOVA were conducted in ARLEQUIN 3.01 and significances of F statistics were estimated using 10 000 nonparametric data permutations (Excoffier *et al*. 2005). Single-locus AMOVA tests were performed to ensure that multilocus results were not affected unduly by one locus. Pairwise F_{ST} and R_{ST} values were estimated for 78 comparisons between 13 locations and three comparisons between regions. Significance levels for multiple comparisons between pairs of samples, or between loci across samples, were adjusted using sequential Bonferroni corrections (Rice 1989).

Standardized measures of genetic divergence. Standardized genetic differentiation measures were obtained by calculating the maximum values of F statistics and dividing the original divergence measures (from the data) by their maximum values, thereby standardizing divergence measures to range from zero to one (Hedrick 2005; Meirmans 2006). Maximum values for F statistics were calculated using the pragmatic recoding approach suggested by Meirmans (2006). Two recoded data sets were constructed. For the first data set, the original data were recoded such that each location had unique alleles. This data set was used to calculate maximum pairwise F_{ST} values between locations. For the second data set, the original data were recoded such that each region had unique alleles. These data were used to calculate maximum F statistics for the hierarchical AMOVA.

Bayesian clustering analyses

Population structure was investigated further, using Bayesian clustering implemented in STRUCTURE 2.2 (Pritchard *et al*. 2000), which identifies the affinities of individual multilocus genotypes to genetic populations and aims to delineate populations that are, as far as possible, in Hardy–Weinberg and linkage equilibrium (Evanno *et al*. 2005). Analyses were run using the default settings [admixture model, correlated allele frequencies among populations, allele frequency distribution parameter (λ) set to 1, and admixture parameter (α) inferred from the data] recommended for STRUCTURE as most powerful for detecting subtle population subdivision (Falush *et al*. 2003). Initial analyses comprised long runs (burn-in = 50 000; MCMC = 1 000 000) replicated three times to ensure convergence on parameters and likelihood values. Shorter runs (burn-in = 20 000; MCMC = 50 000) produced results consistent with long runs and were used for subsequent analyses. Analyses were conducted with and without prior population information for individuals. Analyses incorporating population priors were used to identify recent migrants based on the probability of each individual's membership to clusters. Outputs from STRUCTURE analyses were graphed using DISTRUCT (Rosenberg 2004).

Two criteria were used to identify the most likely number of true populations (K) among *A. laevis* individuals: (i) the value of K with the maximum posterior probability given the data, $\Pr(X/K)$, typically used for STRUCTURE analyses (Pritchard *et al*. 2000); and (ii) $\triangle K$, the maximum second order rate of change of $\Pr(X/K)$ standardized by the standard deviation of $\Pr(X/K)$ (Evanno *et al*. 2005), with the mean and standard deviation of $\Pr(X/K)$ and $\triangle K$ calculated from 20 replicate analyses for each value of K. In systems with hierarchical population structure, STRUCTURE typically best resolves the highest level of population subdivision (Evanno *et al*. 2005). Thus, in order to resolve lower levels of subdivision, STRUCTURE analyses were also conducted separately for each region. Short chains produced variable results for regional analyses; thus, these analyses were conducted using longer runs (burn-in = 50 000; MCMC = 500 000). For all sets of analyses, the number of K values tested was the number of sampled locations plus two.

Isolation by distance. Mantel tests of correlations between genetic and geographical distance matrices, implemented in the Isolation by Distance Web Service 3.11 (IBDWS) (Jensen *et al*. 2005), were used to test for significant relationships between genetic and geographical distance matrices. Mantel tests were conducted using two sets of genetic distances, $F_{ST}/1 - F_{ST}$ and $R_{ST}/1 - R_{ST}$ (Rousset 1997), in order to explore whether genetic distances based on the IAM or the SMM model were better correlated with geographical distances. Geographical distances were measured as the shortest over-water distances between pairs of locations and $\log_{10}$-transformed prior to analyses (Slatkin 1993). A global isolation-by-distance (IBD) analysis was conducted across

all locations and separate analyses were conducted for each geographical region. The significance of each test was assessed using 30 000 data randomizations.

Tests for gender-biased dispersal. Three approaches were used to test for gender-biased dispersal. (i) Gender-specific hierarchical AMOVA were conducted for microsatellites (based on IAM) and mtDNA. Although mtDNA is maternally inherited, it has been used to demonstrate male-biased dispersal (O'Corry-Crowe *et al*. 1997; Escorza-Trevino & Dizon 2000) based on the following rationale: males do not transmit mtDNA haplotypes to subsequent generations; thus, a male immigrants' haplotype is only transiently available for sampling (while it is alive). Reproductive female immigrants do transmit their haplotypes to subsequent generations, thereby having far greater potential to homogenize mtDNA genetic structure by dispersal than males. Stronger mtDNA genetic structure for females than males thus provides compelling evidence for male-biased dispersal (O'Corry-Crowe *et al*. 1997). Small sample sizes necessitated the following groupings: males from Groote and Mornington Islands (GoC); females from Mystery and DJ reefs (Swain Reefs, GBR); and females from Hibernia and Cartier reefs (WA). (ii) Modified multilocus population assignment tests were conducted for each region and for eight locations with adequate sample sizes (at least six individuals of each gender) using GENALEX version 6.0 (Peakall & Smouse 2006). This method produces an assignment index correction (*AIc*) value for males and females at each location or region (Mossman & Waser 1999). Migrants are characterized by negative *AIc* values whereas nonmigrants are characterized by positive *AIc* values. Wilcoxon's signed rank tests were used to test differences in mean *AIc* values for each gender in each region or location. (iii) mtDNA haplotype distributions at Keppel Island and the Swain reefs, southern GBR, were examined for evidence of male-biased dispersal as follows: each of these two locations had one unique but very common haplotype (Swain Reefs, ALH03; Keppel Island, ALH01) and did not share rare haplotypes. However, two Keppel Island individuals had the common Swain Reefs haplotype and three Swain Reefs individuals had the common Keppel Island haplotype (see Figures 3 and 4 in Lukoschek *et al*. 2007b). If these individuals had been males, they may have been recent migrants, thereby supporting male-biased dispersal.

Results

Microsatellite variation, Hardy–Weinberg equilibrium and linkage disequilibrium

Total number of alleles per locus for 330 individuals genotyped at a minimum of four loci ranged from two to 14 (mean = 8.4). All loci had unimodal allele frequency distributions and, with the exception of AL093, one or two very common alleles of intermediate fragment length and some rare alleles. AL093 was the most variable locus and had six alleles of intermediate size that each occurred in 10–20% of chromosomes, plus eight alleles that occurred at low frequencies. Replicate genotyping produced consistent results. Expected and observed heterozygosities ranged from 0.263 to 0.881 and 0.222–0.847, respectively (Table 1). After Bonferroni adjustment of alpha single-locus, exact tests found departures from HWE in eight of 65 within-location tests (initial $\alpha = 0.0083$); in four of 15 within-region tests; and in three loci across all locations (Table 1). The locus AL104_f6 accounted for most departures from HWE, invariably exhibiting heterozygote deficit, probably due to null alleles. To ensure that null alleles did not affect multilocus AMOVA, F_{ST} and R_{ST} estimates, and STRUCTURE analyses, these tests also were conducted with AL104_f6 excluded. Significant LD occurred in two of 130 tests within locations, none of 30 tests within regions, and three of 10 global tests (Table 1). Given the lack of significant LD within locations or regions, global allelic correlations among some loci is probably attributable to population subdivision rather than physical linkage among loci.

Patterns of population subdivision

Hierarchical AMOVA based on variances in allele frequencies (IAM – F_{ST}) revealed highly significant population subdivision at all levels (Table 2), with ~8% of genetic variation attributable to differences among regions. By contrast, AMOVA based on variances in allele size (SMM – R_{ST}) partitioned ~1.5% of genetic variation among regions ($P = 0.139$). Most of the genetic variation (> 90%) was within locations for both the IAM and the SMM. The small proportion of genetic variation due to differences among locations within regions was significant for both mutational models (Table 2). AMOVA with the locus AL104_f6 excluded recovered similar variance partitions and significance levels (results not shown) indicating that possible null alleles did not unduly affect estimates of genetic structure. Single-locus AMOVA based on the IAM (Table 2) and the SMM (results not shown) differed slightly for higher levels of population subdivision but all loci showed highly significant differentiation across locations.

Global genetic structure based on the IAM model also revealed stronger subdivision than the SMM ($F_{ST} = 0.059$, $P < 0.0001$: $R_{ST} = 0.029$, $P < 0.0013$). Similarly, pairwise F_{ST} estimates between locations (mean 0.061 ± 0.023 SE) were generally larger than corresponding R_{ST} estimates (mean 0.023 ± 0.005 SE) (Table 3). This result was largely driven by comparisons between locations in different regions, which generally had much larger F_{ST} than R_{ST} values (mean F_{ST} 0.085 ± 0.007 SE cf. mean R_{ST} 0.028 ± 0.005 SE) (Table 3). By contrast, F_{ST} and R_{ST} values tended to be similarly low

Table 2 Hierarchical AMOVA for *Aipysurus laevis* from 13 locations in three regions (Great Barrier Reef, Gulf of Carpentaria and Western Australia). Results shown for multilocus AMOVA based on variance in allele frequencies (IAM) and allele sizes (SMM); mitochondrial DNA (mtDNA) from Lukoschek *et al*. (2007b); and single-locus AMOVA based on the IAM. All *P* values based on 10 000 Markov chain permutations. *F*(std) are *F* statistics standardized to a range of 0–1 using the methodology of Meirmans (2006)

	All loci IAM			All loci SMM		mtDNA	Al106_d11			AL105_c4			AL28_h4			Al104_f6			AL093		
Source of variation	*F*	*P*	*F*(std)	*F*	*P*	Φ_{ST}	*F*	*P*	*F*(std)	*F*	*P*	*F*(std)	*F*	*P*	*F*(std)	*F*	*P*	*F*(std)	*F*	*P*	*F*(std)
Among regions F_{CT}	0.076	0.001	0.163	0.015	0.139	0.639	0.243	0.001	0.318	0.055	0.016	0.093	0.063	0.006	0.115	0.111	0.001	0.395	0.004	*0.082*	0.033
Among locations in regions F_{SC}*	0.011	0.001	1.000	0.020	0.018	0.447	–0.008	0.919	1.000	0.032	0.001	1.000	0.010	0.142	1.000	0.028	0.001	1.000	0.009	*0.011*	1.000
Within locations F_{ST}	0.087	0.001	0.183	0.035	0.002	0.800	0.237	0.001	0.311	0.086	0.001	0.141	0.073	0.001	0.131	0.136	0.001	0.451	0.013	*0.001*	0.099

*The original and recoded data sets for the hierarchical AMOVA had the same distributions of alleles among locations within regions; thus, F_{SC} values were identical for both data sets resulting in standardized *F* values equaling one for this level of analysis. This result is an artefact of the methodology used to calculate standardized *F* values and this level of analysis is not discussed further.

within regions (mean F_{ST} 0.008 ± 0.003 SE cf. mean R_{ST} 0.013 ± 0.006 SE), with the exception of WA, where some R_{ST} values were larger than corresponding F_{ST} values (Table 3). Theoretical expectations suggest that F_{ST} values will be larger than R_{ST} for recently diverged populations (Gaggiotti *et al*. 1999; Balloux & Lugon-Moulin 2002) consistent with the relatively recent large-scale range expansions by *Aipysurus laevis* into shallow-water habitats around northern Australia.

Thirty-seven pairwise F_{ST} values between locations were significant at $P = 0.05$ and 27 remained significant after Bonferroni correction (initial $\alpha = 0.0006$), whereas 23 pairwise R_{ST} values were nominally significant and none remained significant after adjustment of alpha (Table 3). Most significant F_{ST} values involved comparisons between WA and either the GBR or GoC and only two comparisons between GBR and GoC locations were significant after adjustment of alpha (Table 3). Within-region pairwise F_{ST} values were largest in WA, where most were nominally significant; however, only the Ashmore vs. Scott Reef comparison remained significant after adjustment of alpha (Table 3). Small sample sizes for Cartier and Hibernia reefs probably reduced statistical power for comparisons involving these locations.

Regional F_{ST} and R_{ST} values were highly significant, with the exception of one anomalous small R_{ST} value for WA vs. GBR (Table 4). F_{ST} values for comparisons with WA were larger than R_{ST}, whereas R_{ST} was larger than F_{ST} for GBR vs. GoC (Table 4).

Regional patterns of genetic diversity

Standardized allelic richness and gene diversity across all loci was highest in WA, intermediate in the GoC, and lowest in the GBR (Table 5). This pattern was driven by significantly larger allelic richness and gene diversities in WA at the loci AL106_d11, AL104_f6 and AL105_c4 (Table 5). The pattern of highest microsatellite genetic diversity in WA was consistent with haplotypic and nucleotide diversities found for mtDNA (Table 5).

Standardized estimates of genetic differentiation and comparison with mtDNA

The standardized multilocus F_{CT} was 0.163 and F_{ST} was 0.183 (Table 2). Corresponding mtDNA Φ_{CT} and Φ_{ST} estimates from Lukoschek *et al*. (2007b) were 0.639 and 0.800 (Table 2). Thus, standardized multilocus F_{CT} and F_{ST} estimates were approximately fourfold smaller than mtDNA estimates. Similarly, the standardized global multilocus F_{ST} (0.147) was approximately four times smaller than global mtDNA Φ_{ST} (0.779) (Lukoschek *et al*. 2007b). Standardized regional pairwise F_{ST} estimates between WA and either the GBR or GoC were ~2.5 times smaller than the corresponding

Table 3 Pairwise F_{ST} (below diagonal) and R_{ST} (above diagonal) values for 78 pairwise comparisons between 13 locations for *Aipysurus laevis*. Values in bold in cells shaded grey indicate significant comparisons after sequential Bonferroni correction for multiple comparisons. Values in bold with an asterisk were significant at $P = 0.05$ but not after sequential Bonferroni corrections. All other comparisons were not significant. Significance was tested with 10 000 permutations

	Cent	KpI	DJ	Myst	Thd	Wtip	Grt	Morn	Vand	Cart	Ash	Hib	Scott
Great Barrier Reef													
Central GBR		–0.034	–0.032	–0.001	–0.030	0.004	–0.001	0.003	0.004	–0.010	–0.018	0.022	0.020
Keppel Island	–0.002		0.001	0.023	–0.023	**0.034***	–0.008	–0.007	0.009	–0.008	0.020	0.028	**0.040***
DJ Reef	0.005	0.001		**0.083***	–0.041	**0.090***	–0.022	–0.021	–0.026	–0.064	–0.020	–0.057	**0.065***
Mystery Cay	–0.010	0.008	**0.023***		0.008	–0.018	**0.066***	0.072	**0.068***	**0.088***	0.029	0.079	–0.013
Turtlehead Reef	–0.011	0.006	–0.004	0.001		0.017	0.026	0.041	**0.037***	0.042	**0.036***	0.076	**0.052***
Whitetip Reef	–0.012	0.007	0.004	–0.001	–0.003		**0.064***	0.066	**0.089***	**0.091***	**0.043***	**0.100***	–0.003
Gulf of Carpentaria													
Groote Eylandt	–0.004	0.016	–0.010	**0.027***	0.009	0.004		–0.045	–0.037	–0.012	**0.081***	–0.003	**0.076***
Mornington Island	–0.011	–0.005	–0.005	0.005	–0.001	–0.012	–0.025		–0.046	–0.026	0.083	–0.009	0.075
Vanderlin Island	0.022	**0.018***	–0.013	**0.038**	**0.026***	**0.025**	–0.011	–0.014		–0.013	**0.090***	–0.003	**0.084***
Western Australia													
Cartier Islet	**0.142**	**0.154**	**0.173**	**0.200**	**0.162**	**0.158**	**0.110**	0.110*	**0.094**		0.056	0.012	**0.099***
Ashmore Reef	**0.107**	**0.125**	**0.097**	**0.155**	**0.111**	**0.113**	**0.076**	**0.101**	**0.064**	**0.036***		**0.074***	**0.048***
Hibernia Reef	**0.138**	**0.157**	**0.135**	**0.194**	**0.134**	**0.135**	**0.083**	0.103*	**0.073**	**0.045***	–0.003		0.058
Scott Reef	**0.134**	**0.140**	**0.106**	**0.172**	**0.146**	**0.127**	**0.077**	**0.090**	**0.063**	**0.054***	**0.048**	**0.041***	

NB: individual from Broome not included in pairwise comparisons.

Table 4 Pairwise F_{ST} and R_{ST} values for regional differentiation in *Aipysurus laevis*. Values in bold type were significant at $P = 0.05$ and after Bonferroni correction. Also presented are standardized F_{ST} [F(std)] and corresponding mtDNA Φ_{ST} estimates

	F_{ST}	R_{ST}	F(std)	Φ_{ST}
Great Barrier Reef vs. Gulf of Carpentaria	**0.018**	**0.036**	0.039	**0.787**
Western Australia vs. Great Barrier Reef	**0.126**	0.001	0.305	**0.679**
Western Australia vs. Gulf of Carpentaria	**0.066**	**0.056**	0.189	**0.510**

Table 5 Regional allelic richness, number of alleles per locus standardized to a sample size of 20 (Ns), and gene diversity weighted by regional sample size (Hs) for *Aipysurus laevis*. Significance tests were based on 15 000 permutations. Values in bold indicate significant differences at $P = 0.05$. Comparisons are indicated as follows: *GBR vs. GoC; †GBR vs. WA. No comparisons for WA vs. GoC were significantly different. Also presented are corresponding mtDNA haplotypic ($h \pm$ SE) and nucleotide ($\pi \pm$ SE percentage) diversities from Lukoschek *et al*. (2007b)

	AL106_d11	AL105_4	AL28_h4	AL104_f6	AL093	All loci		mtDNA
Great Barrier Reef								
Ns	**1.99***	**2.96†**	1.98	6.08	6.84	**3.25†**	***h***	0.55 ± 0.03
Hs	**0.069†**	**0.297†**	0.440	**0.613†**	0.882	**0.456†**	π	0.12 ± 0.10
Gulf of Carpentaria								
Ns	**4.23***	3.50	1.99	5.69	5.81	3.44	***h***	0.58 ± 0.07
Hs	0.337	0.428	0.430	0.749	0.871	0.568	π	0.18 ± 0.13
Western Australia								
Ns	3.00	**4.77†**	1.99	9.43	6.40	**4.05†**	***h***	0.63 ± 0.03
Hs	**0.567†**	**0.597†**	0.473	**0.848†**	0.879	**0.661†**	π	0.52 ± 0.30

mtDNA Φ_{ST} estimates. In stark contrast, the standardized microsatellite F_{ST} for GBR vs. GoC (0.039) was ~20 times smaller than mtDNA Φ_{ST} (0.787) (Table 4).

Many pairwise F_{ST} estimates between locations had negative values (Table 3), which produced large negative standardized values. Meirmans (2006) recommended that negative F_{ST} estimates be converted to standardized divergences of zero; thus, standardized pairwise F_{ST} values for comparisons involving WA locations ranged from zero to 0.481 (mean = 0.282), while corresponding mtDNA Φ_{ST}

Table 6 Standardized multilocus pairwise F_{ST} estimates (below diagonal) and Φ_{ST} estimates from mitochondrial ND4 sequence data (above diagonal) for 78 pairwise comparisons between 13 locations for *Aipysurus laevis*. Standardized microsatellite divergence estimates were calculated following the methodology of Meirmans (2006) and mitochondrial estimates were calculated as described in Lukoschek *et al*. (2007b)

	Cent	KpI	DJ	Myst	Thd	Wtip	Grt	Morn	Vand	Cart	Ash	Hib	Scott
Central GBR		0.438	0.401	0.637	0.581	0.724	0.304	0.703	0.764	0.867	0.513	0.410	0.770
Keppel Island	0.000		0.595	0.747	0.714	0.799	0.705	0.907	0.893	0.953	0.696	0.782	0.896
DJ Reef	0.012	0.003		–0.003	0.021	0.029	0.674	0.813	0.844	0.907	0.716	0.734	0.851
Mystery Cay	0.000	0.015	0.047		0.008	0.011	0.744	0.927	0.916	0.957	0.735	0.813	0.914
Turtlehead Reef	0.000	0.014	0.009	0.000		0.034	0.731	0.902	0.901	0.943	0.718	0.791	0.900
Whitetip Reef	0.000	0.012	0.000	0.002	0.000		0.772	0.950	0.932	0.967	0.751	0.837	0.930
Groote Eylandt	0.000	0.000	0.000	0.011	0.000	0.000		–0.061	–0.031	0.296	0.441	0.333	0.499
Mornington Island	0.000	0.034	0.000	0.056	0.019	0.009	0.000		0.020	0.362	0.498	0.405	0.585
Vanderlin Island	0.046	0.039	0.000	0.081	0.058	0.055	0.000	0.000		0.429	0.513	0.458	0.568
Cartier Islet	0.260	0.304	0.263	0.362	0.278	0.273	0.206	0.251	0.179		0.322	0.676	0.918
Ashmore Reef	0.324	0.360	0.373	0.424	0.318	0.301	0.218	0.257	0.195	0.120		0.276	0.561
Hibernia Reef	0.328	0.361	0.481	0.444	0.391	0.359	0.292	0.270	0.257	0.136	0.000		0.122
Scott Reef	0.357	0.352	0.299	0.415	0.382	0.318	0.228	0.253	0.187	0.185	0.165	0.135	

NB: individual from Broome not included in pairwise comparisons.

estimates (Lukoschek *et al*. 2007b) ranged from 0.122 to 0.967 (mean = 0.657) (Table 6). By contrast, standardized pairwise F_{ST} values within or between the GBR and GoC ranged from zero to 0.081 (mean = 0.014), whereas mtDNA Φ_{ST} estimates ranged from –0.003 to 0.950 (mean = 0.557) (Table 6). On average, standardized microsatellite F_{ST} values involving WA locations were therefore ~2.5 times smaller than corresponding mtDNA Φ_{ST}, whereas comparisons between GBR and/or GoC locations were orders of magnitude lower than their mtDNA Φ_{ST} counterparts (Table 6).

Population structure from Bayesian clustering analyses

STRUCTURE analyses recovered highest posterior probabilities of the data for two [Pr(X/K: 2) = –3651.5] and three [Pr(X/K: 3) = –3634.6] clusters. However, posterior probabilities were similar for other values of K and the variance of Pr(X/K) increased markedly as K increased. It was, therefore, not possible to unequivocally determine the most likely number of *A. laevis* populations using the maximum Pr(X/K) criterion. Analyses with the locus AL104_f6 excluded recovered similar results (not shown). The modal value of $\triangle K$ was at K = 2; however, the rate of change in $\triangle K$ (relative height of modal value) was small, suggesting a weak signal in the data (Evanno *et al*. 2005). Nonetheless, the assignment probabilities of individual genotypes showed evidence of geographical structuring, particularly for WA individuals, which were assigned predominantly to one cluster (Fig. 2a). By contrast, the individuals from the GBR and GoC were not assigned predominantly to either one of the two clusters (Fig. 1a). Analyses incorporating location priors identified four GoC individuals (three males and one female) as potential recent migrants (Fig. 2b). However, three of these individuals had the most common GoC mtDNA haplotype (ALH10) and the fourth individual had the next most common haplotype (ALH12); thus, it is unlikely that they were recent migrants. Assigning individuals to three clusters did not improve geographical structuring for GBR and GoC individuals (results not shown). In addition, separate within-region STRUCTURE analyses did not resolve the most likely number of clusters for any region, using either the maximum Pr(X/K) or the modal $\triangle K$ criteria.

Isolation by distance

The global Mantel test revealed a significant correlation between the $F_{ST}/1 - F_{ST}$ genetic distance and geographical distance matrices (r = 0.556, P < 0.0001), and RMA regression recovered a positive relationship between genetic and geographical distances that explained 30.9% of the variance (Fig. 3a). There were, however, no significant relationships between genetic and geographical distances within WA (r = 0.616, P < 0.123), the GoC (r = –0.963, P ~ 0.50), or the GBR (r = 0.332, P < 0.210), or between genetic distances calculated as $R_{ST}/1 - R_{ST}$ and geographical distances at any level of analysis (Fig. 3b). The regression relationship based on microsatellite allele frequencies had greatly increased variances for genetic distances over the largest geographical scale (between locations in different regions). A similar pattern was also found for mtDNA (Fig. 3c). However, while there was no geographical structuring among corresponding mtDNA $\Phi_{ST}/1 - \Phi_{ST}$ genetic distances (Fig. 3c), microsatellite $F_{ST}/1 - F_{ST}$ distances were clustered by the regional comparisons involved: GBR vs. GoC had

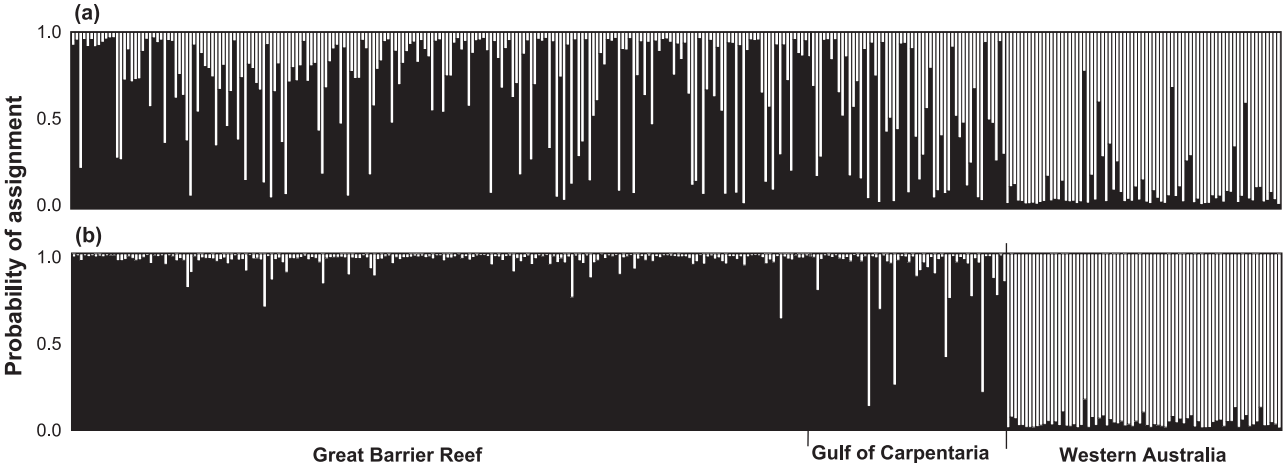

Fig. 2 Clustering of *Aipysurus laevis* individuals from model-based algorithm implemented in STRUCTURE 2.2 (Pritchard *et al*. 2000). Each column along the *x* axis represents one *A. laevis* individual grouped by region and location in the same order as Table 1. The *Y*-axis represents the assignment probability of each individual into two clusters ($K = 2$). (a) Admixture model without population prior. (b) Admixture model with population prior.

the smallest genetic distances, GBR vs. WA had the largest genetic distances, and GoC vs. WA were intermediate (Fig. 3a).

Gender-biased dispersal not supported by nuclear or mitochondrial DNA

AMOVA based on microsatellite allele frequencies had virtually identical genetic structure and hierarchical partitioning of genetic variation for males ($F_{ST} = 0.077$) and females ($F_{ST} = 0.078$), whereas mtDNA recovered stronger genetic structure for males ($\Phi_{ST} = 0.846$) than females ($\Phi_{ST} = 0.726$). In addition, mean *AIc* values were not significantly different for males and females in the three regions and in six of the eight locations tested (Table 7). In the GoC mean *AIc* values at Groote Eylandt were lower for females than for males, suggesting female-biased dispersal, whereas the opposite pattern was found at Vanderlin Island (Table 7). However, *A. laevis* is virtually panmictic with respect to mtDNA in the GoC (Lukoschek *et al*. 2007b) thus this result is most likely a sampling artefact, although may also indicate gender-specific seasonal movement patterns. Finally, evidence that dispersal is not biased towards males comes from the anomalous haplotypes sampled in the Swain Reefs and Keppel Island. The two individuals sampled at Keppel Island carrying the common Swain Reefs haplotype (ALH03) were both females, and one of the three Swain Reefs individuals with the common Keppel Island haplotype (ALH01) was also female. In the absence of paternal leakage (Zouros *et al*. 1992), this result indicates that females with anomalous haplotypes have been either recently dispersed and then sampled, or inherited their haplotypes from females that dispersed in the past. Either scenario indicates that dispersal was by females and not by males. The higher levels of shared haplotypes among locations in WA and the GoC precluded this type of direct inference of female dispersal.

Table 7 Mean (SE) *AIc* values for eight locations and three regions for *Aipysurus laevis*. Sample sizes are ratios of males to females

	Sample size	Males	Females
Keppel Island	23 : 11	–0.01 (0.16)	0.03 (0.31)
Mystery Cay	15 : 14	0.10 (0.20)	–0.10 (0.25)
Turtlehead Reef	14 : 16	0.02 (0.36)	–0.02 (0.25)
Whitetip Reef	19 : 19	0.06 (0.20)	–0.06 (0.28)
Gulf of Carpentaria	25 : 27	–0.10 (0.22)	0.10 (0.22)
Groote Eylandt*	7 : 7	0.40 (0.24)	–0.40 (0.58)
Vanderlin Island†	16 : 16	–0.28 (0.23)	0.28 (0.21)
Western Australia	32 : 25	0.06 (0.15)	–0.08 (0.21)
Ashmore Reef	16 : 10	–0.06 (0.21)	0.10 (0.24)
Scott Reef	6 : 10	0.17 (0.39)	–0.10 (0.23)

*Significantly smaller *AIc* values for females than males;
†Significantly smaller *AIc* values for males than females.

Discussion

Regional patterns of population structure and distribution of genetic diversity for five nuclear microsatellites for *Aipysurus laevis* around northern Australia were broadly congruent with results from mtDNA (Lukoschek *et al*. 2007b). WA reefs had the highest genetic diversities and were more divergent from the GBR and GoC than the latter two regions were from each other. These congruent patterns

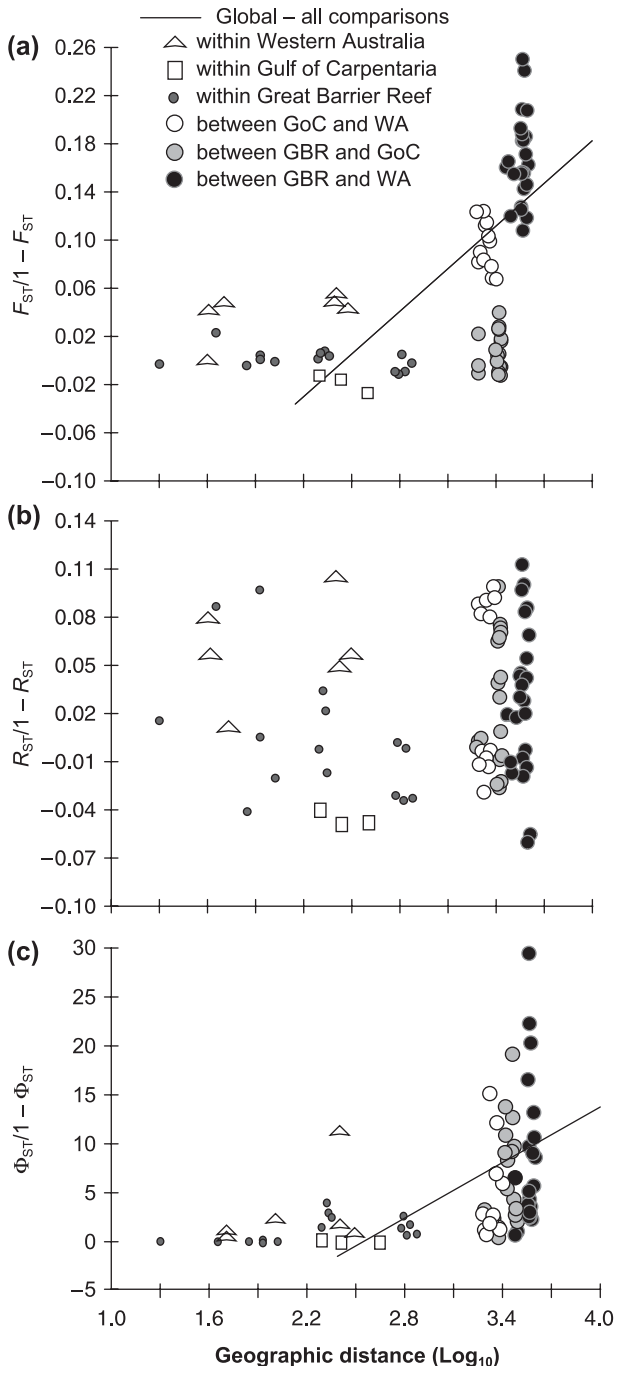

Fig. 3 Reduced major axis regressions showing relationships between *Aipysurus laevis* genetic and geographical distances for all 13 locations (Broome not included) and separately for each region. Comparisons between locations within and between regions are indicated by different symbols shown in the key. (a) Genetic distances based on IAM ($F_{ST}/1 - F_{ST}$). Mantel tests indicated a significant global effect of isolation by distance (IBD) but no IBD within regions. (b) Genetic distances based on SMM ($R_{ST}/1 - R_{ST}$) indicated no significant IBD at any level of analysis. (c) mtDNA genetic distances calculated as $\Phi_{ST}/1 - \Phi_{ST}$ from Lukoschek *et al*. (2007b). Mantel tests indicated significant global IBD but no IBD within regions.

suggest that Pleistocene processes similarly shaped genetic divergence and diversity at nuclear and mitochondrial loci for *A. laevis*. Furthermore, nuclear microsatellites supported the hypothesis (based on mtDNA) that *A. laevis* persisted on WA reefs over numerous glaciation cycles, whereas the GBR and GoC were colonized more recently, probably by west-to-east dispersal (Lukoschek *et al*. 2007b). Despite congruent regional patterns of divergence, the strong hierarchical partitioning of genetic variation among regions and locations for mitochondrial matrilines (Lukoschek *et al*. 2007b) was not found for microsatellites. Instead, most genetic variation for microsatellites occurred at the level of individuals. Nonetheless, standardized microsatellite divergence estimates for comparisons that involved WA (either within WA or between WA and the GBR or GoC) were quantitatively similar to mtDNA (after taking the fourfold difference in effective population sizes between the marker classes into account). By contrast, standardized F_{ST} values within or between the GBR and GoC were orders of magnitude smaller than mtDNA Φ_{ST} estimates. Thus, microsatellites did not perform better than mtDNA at smaller geographical and shorter temporal scales and did not resolve fine-scale patterns of population structure within the GBR or GoC.

Comparison between mtDNA and microsatellite markers and gender-biased dispersal

Despite much lower genetic divergences for nuclear than mtDNA over small (within regions) and intermediate (between the GBR and GoC) spatial scales (Table 6), male-biased dispersal by *A. laevis* was not supported by tests of the genetic data. Hierarchical AMOVA recovered almost identical partitions of genetic variation for males and females for both marker classes. Mean *AIc* values were generally not significantly different for males and females (Table 7), and the five individuals with anomalous mtDNA haplotypes at Keppel Island and the Swain Reefs (i.e. the common haplotype of the other location) comprised three females and two males, suggesting either that: (i) both genders occasionally disperse between these locations; (ii) females dispersed in the past and transmitted their haplotypes to male and female descendants; or (iii) the aberrant haplotypes reflect remnant ancestral polymorphisms. Although clustering analyses with population-priors detected potential recent migrants between regions (Fig. 2b), mitochondrial data did not support recent migration by these snakes, which probably had anomalous multilocus genotypes that were difficult to assign. Interestingly, the genetic data are not consistent with a preliminary mark–recapture study of *A. laevis* movement patterns, which suggested that males predominantly moved between adjacent Keppel Island reefs (Lynch 2000). However, the very small spatial scale of this mark–recapture study

(< 10 km) precludes meaningful comparison with the molecular data. Field estimates of male and female dispersal over distances comparable to our estimates of gene flow (50–500 km) would, however, be challenging to obtain, given the complex logistics of directly estimating dispersal for cryptic marine species and the generally low dispersal of *A. laevis* predicted from mtDNA (Lukoschek *et al*. 2007b). Moreover, occasional 'chance' dispersal events by males and females (during storms) may result in discrepancies between estimates of dispersal from field and genetic data.

Multiple tests refuting male-biased dispersal provided compelling evidence that the stronger partitioning of mitochondrial than nuclear genetic diversity was not the result of male-biased dispersal. These differences must therefore be accounted for by marker-specific mutation rates, modes of inheritance, and genomic sampling variances (Birky *et al*. 1983, 1989). Buonaccorsi *et al*. (2001) used simulations to show that populations with identical (simulated) histories can differ substantially with respect to the means and variances of F_{ST} estimates for nuclear and mitochondrial markers. Specifically, sampling variance (genetic drift) resulted in larger variances among F_{ST} estimates for mitochondrial than nuclear markers, particularly when migration rates were low and/or effective population sizes (N_{em}) were small (Buonaccorsi *et al*. 2001). Indeed, for simulated values of $N_{em} = 1$, 95% CI of F_{ST} estimates for nuclear markers ranged from 0.05 to 0.15, whereas for mtDNA, 95% CI of F_{ST} ranged from 0.0006 to 0.70 (Buonaccorsi *et al*. 2001). Although F_{ST} estimates for *A. laevis* are not directly comparable with simulated values from Buonaccorsi *et al*. (2001), global F_{ST} estimates for microsatellites (0.059) and mtDNA (0.610) fall within the simulated 95% CIs for nuclear and mitochondrial markers. In addition, standardizing F statistics (to maximum values of one) resulted in global divergence estimates and pairwise comparisons involving WA that were two to four times smaller than corresponding mtDNA divergence estimates (Tables 2, 3 and 6). This difference is consistent with the fourfold larger effective population sizes for nuclear than mitochondrial markers (Birky *et al*. 1983; Buonaccorsi *et al*. 2001). Thus, mtDNA and microsatellites gave congruent divergence estimates for comparisons involving WA locations, which were also consistent with the genetic distinctiveness of WA individuals indicated by Bayesian clustering analyses (Fig. 2).

Evolutionary perspectives

Congruent patterns of strong regional differentiation (Tables 2, 4 and 6) and higher genetic diversity in WA than the GoC and GBR (Table 5), revealed by the conjoint use of microsatellite and mtDNA markers, support the hypothesis of longer-term persistence of *A. laevis* on WA reefs relative to the recent colonization of the GBR and GoC (Lukoschek *et al*. 2007b). In addition, similar levels of divergence for mtDNA and microsatellites among WA locations (Table 6) suggest that gene flow between WA reefs has been restricted for sufficient time to allow divergence at both mtDNA and nuclear loci (Birky *et al*. 1983). Despite the predicted higher information content of microsatellite markers, the five loci used in this study did not improve resolution of population structure for younger populations within or between the GBR and GoC. In particular, the strong mtDNA subdivision between the GBR and GoC (which did not share mtDNA haplotypes) and between Keppel Island, the Swain Reefs in the GBR (Lukoschek *et al*. 2007b) was not found for nuclear microsatellites (Tables 3 and 4). This anomaly may be explained by the recent independent colonization of these locations by *A. laevis* lineages with divergent mtDNA haplotypes but similar microsatellite allele frequencies. In addition, microsatellites perform best for populations with constant and relatively small sizes (Queney *et al*. 2001). Recent population expansions over short evolutionary times, combined with the typically large contemporary populations sizes of *A. laevis* (Burns 1984), suggest that GBR and GoC have not reached mutation–drift equilibrium for nuclear loci and populations in these regions may still be in the process diverging (Hellberg 1994).

The structured pattern of microsatellite genetic distances ($F_{ST}/1 - F_{ST}$) between locations in different regions (Fig. 3a) further support the colonization of the GoC and GBR by *A. laevis* via west-to-east dispersal. Genetic distances were smallest between the GBR and GoC, highlighting their recent ancestral affinities. However, genetic distances between WA and the GoC (adjacent regions) were smaller than between the geographically distant WA and the GBR (Fig. 3a), suggesting west-to-east range expansion along a geographical gradient. Interestingly, mtDNA $\Phi_{ST}/1 - \Phi_{ST}$ distances between locations in different regions were not geographically structured (Fig. 3c), possibly the result of the high sampling variances shown to occur for mtDNA F_{ST} estimates (Buonaccorsi *et al*. 2001).

Regional microsatellite divergence estimates were larger for F_{ST} than R_{ST} consistent with recent divergence among populations (Gaggiotti *et al*. 1999; Balloux & Lugon-Moulin 2002). A similar pattern of larger F_{ST} than R_{ST} estimates was found for green turtles, *Chelonia mydas*, around northern Australia (FitzSimmons *et al*. 1997b). Despite Fitzsimmons *et al*. (1997b) attributing this result to low microsatellite mutation rates, stronger regional F_{ST} than R_{ST} for *A. laevis* and *C. mydas* may reflect their recent large-scale range expansions into shallow-water habitats in the GBR and GoC, which occurred subsequent to marine transgressions of Australia's continental shelf less than 10 000 years ago (Torgersen *et al*. 1985). Further genetic studies of marine populations around northern Australia are required to evaluate the generality of this pattern.

Conclusions

Historical and contemporary processes have shaped regional patterns of genetic diversity and divergence for *Aipysurus laevis* around northern Australia at both microsatellite and mitochondrial loci. Nonetheless the predicted high discriminatory power of microsatellites for resolving population structure between geographically proximate populations with shallow evolutionary divergences (Goudet *et al*. 1996; Buonaccorsi *et al*. 1999) was not found for the five *A. laevis* microsatellite loci used in this study (Tables 4 and 6). The combined used of three approaches to test for gender-biased dispersal rejected the hypothesis that the generally weaker genetic subdivision at nuclear than mitochondrial markers was the result of male-biased gene flow. This result highlights the importance of rigorously testing the hypothesis of gender-biased dispersal. Results from recently described approaches for standardizing divergence estimates for levels of polymorphism and Bayesian clustering analyses confirmed the genetic distinctiveness of *A. laevis* on WA reefs compared with the GBR and GoC, previously documented for mtDNA, which has significant conservation implications for this species (discussed in Lukoschek *et al*. 2007b). This study highlights the importance of critically evaluating patterns and levels of genetic differentiation inferred from microsatellite markers in the context of the potentially complex intraspecific evolutionary histories and population dynamics of the study species and the effects of palaeoclimatic processes in the study region.

Acknowledgements

This study was funded by the CRC for Reef Research. V.L. was supported by APA and CRC Postgraduate Scholarships. We thank P. Doherty, AIMS, the Australian Customs Service and DEH for in-kind ship-time to collect samples. CSIRO provided the GoC tissue samples. We thank C. Dudgeon, E. Hutchison, and S. Lowe for assistance in the field. J. Avise and C. Riginos provided helpful comments on early drafts of the manuscript. This research was conducted under JCU Animal Ethics Permit A653_01, GBRMPA Permit G01/224 and EA Permit E2002/0031.

References

Allendorf FW, Seeb LW (2000) Concordance of genetic divergence among sockeye salmon populations at allozyme, nuclear DNA, and mitochondrial DNA markers. *Evolution*, **54**, 640–651.

Angers B, Bernatchez L (1998) Combined use of SMM and non-SMM methods to infer fine structure and evolutionary history of closely related brook charr (*Salvelinus fontinalis*, Salmonidae) populations from microsatellites. *Molecular Biology and Evolution*, **15**, 143–159.

Avise JC (2000) *Phylogeography: The History and Formation of Species*. Harvard University Press, Cambridge, Massachusetts.

Ballard JWO, Kreitman M (1995) Is mitochondrial DNA a strictly neutral marker? *Trends in Ecology & Evolution*, **10**, 485–488.

Balloux F, Goudet J, Perrin N (1998) Breeding system and genetic variance in the monogamous, semi-social shrew, *Crocidura russula*. *Evolution*, **52**, 1230–1235.

Balloux F, Brunner H, Lugon-Moulin N, Hausser J, Goudet J (2000) Microsatellites can be misleading: an empirical and simulation study. *Evolution*, **54**, 1414–1422.

Balloux F, Lugon-Moulin N (2002) The estimation of population differentiation with microsatellite markers. *Molecular Ecology*, **11**, 155–165.

Birky CW, Maruyama T, Fuerst PA (1983) An approach to population and evolutionary genetic theory for genes in mitochondria and chloroplasts, and some results. *Genetics*, **103**, 513–527.

Birky CW, Fuerst PA, Maruyama T (1989) Organelle gene diversity under migration, mutation and drift: equilibrium expectations, approach to equilibrium, effects of heteroplasmic cells, and comparison to nuclear genes. *Genetics*, **121**, 613–627.

Brown WM, George MJ, Wilson AC (1979) Rapid evolution of animal mitochondrial DNA. *Proceedings of the National Academy of Sciences USA*, **76**, 1967–1971.

Buonaccorsi VP, Reece KS, Morgan LW, Graves JE (1999) Geographic distribution of molecular variance within the blue marlin (*Makaira nigricans*): a hierarchical analysis of allozyme, single-copy nuclear DNA, and mitochondrial DNA markers. *Evolution*, **53**, 568–579.

Buonaccorsi VP, McDowell JR, Graves JE (2001) Reconciling patterns of inter-ocean molecular variance from four classes of molecular markers in blue marlin (*Makaira nigricans*). *Molecular Ecology*, **10**, 1179–1196.

Burns GW (1984) *Aspects of population movements and reproductive biology of* Aipysurus laevis, *the olive sea snake*. PhD, University of New England.

Castella V, Ruedi M, Excoffier L (2001) Contrasted patterns of mitochondrial and nuclear structure among nursery colonies of the bat *Myotis myotis*. *Journal of Evolutionary Biology*, **14**, 708–720.

Davies P (1994) Evolution of the Great Barrier Reef. *Australian Geologist*, **92**, 21–24.

Eizerik E, Kim J-H, Menotti-Raymond M *et al*. (2001) Phylogeography, population history and conservation genetics of jaguars (*Panthera onca*, Mammalia, Felidae). *Molecular Ecology*, **10**, 65–79.

Escorza-Trevino S, Dizon AE (2000) Phylogeography, intraspecific structure and sex-biased dispersal of Dall's porpoise, *Phocoenoides dalli*, revealed by mitochondrial and microsatellite DNA analysis. *Molecular Ecology*, **9**, 1049–1060.

Estoup A, Angers B (1998) Microsatellites and minisatellites for molecular ecology: theoretical and empirical considerations. In: *Advances in Molecular Ecology* (Ed. by Carvalho GR), pp. 55–86. IOS Press, Amsterdam.

Estoup A, Garnery L, Solignac M, Cornuet JM (1995) Microsatellite variation in honey bee (*Apis mellifera* L.) populations: hierarchical genetic structure and test of the infinite allele and stepwise mutation models. *Genetics*, **140**, 679–695.

Estoup A, Jarne P, Cornuet JM (2002) Homoplasy and mutation model at microsatellite loci and their consequences for population genetics analysis. *Molecular Ecology*, **11**, 1591–1604.

Evanno G, Regnaut S, Goudet J (2005) Detecting the number of clusters of individuals using the software STRUCTURE: a simulation study. *Molecular Ecology*, **14**, 2611–2620.

Excoffier L, Laval G, Schneider S (2005) ARLEQUIN (version 3.0): an integrated software package for population genetics data analysis. *Evolutionary Bioinformatics Online*, **1**, 47–50.

Falush D, Stephens M, Pritchard JK (2003) Inference of population structure using multilocus genotype data: linked loci and correlated allele frequencies. *Genetics*, **164**, 1567–1587.

Favre L, Balloux F, Goudet J, Perrin N (1997) Female-biased dispersal in the monogamous mammal *Crocidura russula*: evidence from field data and microsatellite patterns. *Proceedings of the Royal Society B: Biological Sciences*, **264**, 127–132.

FitzSimmons NN, Limpus CJ, Norman JA *et al*. (1997a) Philopatry of male marine turtles inferred from mitochondrial DNA markers. *Proceedings of the National Academy of Sciences, USA*, **94**, 8912–8917.

FitzSimmons NN, Moritz C, Limpus CJ, Pope L, Prince R (1997b) Geographic structure of mitochondrial and nuclear gene polymorphism in Australian green turtle populations and male-biased gene flow. *Genetics*, **147**, 1843–1854.

Gaggiotti OE, Lange O, Rassmann K, Gliddons C (1999) A comparison of two indirect methods for estimating average levels of gene flow using microsatellite data. *Molecular Ecology*, **8**, 1513–1520.

Goudet J (2001) FSTAT, *a Program to Estimate and Test Gene Diversities and Fixation Indices* (Version 2.9.3). Available from http://www.unil.ch/izea/softwares/fstat.html.

Goudet J, Raymond M, de Meeus T, Rousset F (1996) Testing differentiation in diploid populations. *Genetics*, **139**, 463–471.

Guo SW, Thompson EA (1992) Performing the exact test of Hardy–Weinberg proportion for multiple alleles. *Biometrics*, **48**, 361–372.

Heatwole H (1999) *Sea Snakes*, 2nd edn. University of New South Wales Press, Sydney.

Hedrick PW (1999) Highly variable loci and their interpretation in evolution and conservation. *Evolution*, **53**, 313–318.

Hedrick PW (2005) A standardized genetic differentiation measure. *Evolution*, **59**, 1633–1638.

Hellberg ME (1994) Relationships between inferred levels of gene flow and geographic distance in a philopatric coral, *Balanophyllia elegans. Evolution*, **48**, 1829–1854.

Hewitt GM (2000) The genetic legacy of the Quaternary ice ages. *Nature*, **405**, 907–913.

Jensen JL, Bohonak AJ, Kelley ST (2005) Isolation by distance, web service. *Biomedical Central Genetics*, **6**, 13–18.

Johnson JA, Toepfer JE, Dunn PO (2003) Contrasting patterns of mitochondrial and microsatellite population structure in fragmented populations of greater prairie-chickens. *Molecular Ecology*, **12**, 3335–3347.

Karl SA, Bowen BW, Avise JC (1992) Global population structure and male-mediated gene flow in the green turtle (*Chelonia mydas*): RFLP analyses of anonymous nuclear loci. *Genetics*, **131**, 163–173.

Keeney DB, Heupel MR, Heuter RE, Heist EJ (2005) Microsatellite and mitochondrial DNA analyses of the genetic structure of blacktip shark (*Carcharhinus limbatus*) nurseries in the northwestern Atlantic, Gulf of Mexico, and Caribbean Sea. *Molecular Ecology*, **14**, 1911–1923.

Keogh JS, Webb JK, Shine R (2007) Spatial genetic analysis and long-term mark-recapture data demonstrate male-biased dispersal in a snake. *Biology Letters*, **3**, 33–35.

Lehman TN, Besansky J, Hawley WA (1997) Microgeographic structure of *Anopheles gambiae* in western Kenya based on mtDNA and microsatellite loci. *Molecular Ecology*, **6**, 243–253.

Lukoschek V, Waycott M, Dunshea G (2005) Isolation and characterization of microsatellite loci from the Australasian sea snake, *Aipysurus laevis*. *Molecular Ecology Notes*, **5**, 875–881.

Lukoschek V, Heatwole H, Grech A, Burns G, Marsh H (2007a) Distribution of two species of sea snakes, *Aipysurus laevis* and *Emydocephalus annulatus*, in the southern Great Barrier Reef: metapopulation dynamics, marine protected areas and conservation. *Coral Reefs*, **26**, 291–307.

Lukoschek V, Waycott M, Marsh H (2007b) Phylogeographic structure of the olive sea snake, *Aipysurus laevis* (Hydrophiinae) indicates recent Pleistocene range expansion but low contemporary gene flow. *Molecular Ecology*, **16**, 3406–3422.

Lynch TP (2000) *The behavioural ecology of the olive sea snake, Aipysurus laevis* PhD Thesis, James Cook University, Queensland, Australia.

Meirmans PG (2006) Using the AMOVA framework to estimate a standardized genetic differentiation measure. *Evolution*, **60**, 2399–2402.

Mossman CA, Waser PM (1999) Genetic detection of sex-biased dispersal. *Molecular Ecology*, **8**, 1063–1067.

Natoli A, Peddemors VM, Hoelzel AR (2004) Population structure and speciation in the genus *Tursiops* based on microsatellite and mitochondrial DNA analyses. *Journal of Evolutionary Biology*, **17**, 363–375.

Nei M (1987) *Molecular Evolutionary Genetics*. Columbia University Press, New York.

O'Corry-Crowe GM, Suydam RS, Rosenberg A, Frost KJ, Dizon AE (1997) Phylogeography, population structure and dispersal patterns of the beluga whale, *Delphinapterus leucas*, in the western Nearctic revealed by mitochondrial DNA. *Molecular Ecology*, **6**, 955–970.

Pardini AT, Jones CS, Noble LR *et al*. (2001) Sex-biased dispersal of great white sharks. *Nature*, **412**, 139–140.

Peakall R, Smouse PE (2006) GENALEX 6: genetic analysis in Excel. Population genetic software for teaching and research. *Molecular Ecology Notes*, **6**, 288–295.

Pritchard JK, Stephens M, Donnelly P (2000) Inference of population structure using multilocus genotype data. *Genetics*, **155**, 945–959.

Queney G, Ferrand N, Weiss S, Mougel F, Monnerot M (2001) Stationary distribution of microsatellite loci between divergent population groups of the European rabbit (*Oryctolagus cuniculus*). *Molecular Biology and Evolution*, **18**, 2169–2178.

Rassmann K, Tautz D, Trillmich F, Gliddon C (1997) The microevolution of the Galapagos marine iguana *Amblyrhynchus cristatus* assessed by nuclear and mitochondrial genetic analyses. *Molecular Ecology*, **6**, 437–452.

Raymond M, Rousset F (1995) GENEPOP (version 1.2): population genetics software for exact tests and ecumenicism. *Journal of Heredity*, **86**, 248–249.

Rice WR (1989) Analysing tables of statistical tests. *Evolution*, **43**, 223–225.

Rosenberg NA (2004) DISTRUCT: a program for the graphical display of population structure. *Molecular Ecology Notes*, **4**, 137–138.

Rousset F (1996) Equilibrium values of measures of population subdivision for stepwise mutation processes. *Genetics*, **142**, 1357–1362.

Rousset F (1997) Genetic differentiation and estimation of gene flow from *F*-statistics under isolation by distance. *Genetics*, **145**, 1219–1228.

Shaw PW, Turan C, Wright JM, O'Connell M, Carvalho GR (1999) Microsatellite DNA analysis of population structure in Atlantic herring (*Clupea harengus*), with direct comparison to allozyme and mtDNA RFLP analyses. *Heredity*, **83**, 490–499.

Slatkin M (1993) Isolation by distance in equilibrium and non-equilibrium populations. *Evolution*, **47**, 264–279.

Slatkin M (1995) A measure of population subdivision based on microsatellite allele frequencies. *Genetics*, **139**, 457–462.

Takahashi K, Nei M (1996) Genetic distances and reconstruction of phylogenetic trees from microsatellite DNA. *Genetics*, **114**, 389–399.

Torgersen T, Jones MR, Stephens AW, Searle DE, Ullman WJ (1985) Late Quaternary hydrological changes in the Gulf of Carpentaria. *Nature*, **313**, 785–787.

Wirth T, Bernatchez L (2001) Genetic evidence against panmixia of the European eel. *Nature*, **409**, 1037–1040.

Zouros E, Freeman KR, Ball AO, Pogson GH (1992) Direct evidence for extensive paternal mitochondrial-DNA inheritance in the marine mussel *Mytilus*. *Nature*, **359**, 412–414.

Vimoksalehi Lukoschek is interested in the molecular ecology, evolution and conservation of marine organisms, particularly vertebrates in tropical waters, and biogeographical patterns throughout the Indo-West Pacific. She studied hydrophiine sea snakes for her doctoral dissertation and was supervised by Michelle Waycott, whose research encompasses the molecular ecology and evolution of numerous marine and terrestrial organisms, and Scott Keogh, a herpetologist who researches the molecular ecology and evolutionary biology of a wide range of species.
